Jahn-Teller dynamics of the organic ferromagnet-tetrakis(dimethylamine) ethylene-C_{60}

P. Jeglič,[1] R. Blinc,[1] T. Apih,[1] A. Omerzu,[1] and D. Arčon[1,2]
[1]*Institute Jozef Stefan, Ljubljana, Slovenia*
[2]*Faculty of Mathematics and Physics, University of Ljubljana, Slovenia*
(Received 10 March 2003; revised manuscript received 11 June 2003; published 21 November 2003)

We report on the measurements of the ^{13}C NMR line shape in the organic ferromagnet tetrakis(dimethylamine) ethylene-C_{60} between room temperature and 4 K as well as on a simulation of the line shape in this interval. It is shown that the sudden increase in the inhomogeneous ^{13}C NMR linewidth in the middle of the ferromagnetic phase can be explained by the freezeout of the pseudorotations of the axes of the Jahn-Teller distortions of the C_{60}^- ions. The correlation times for the Jahn-Teller dynamics of the C_{60}^- ions have been extracted from a comparison of experimental and simulated ^{13}C NMR line shapes. A strong correlation between spin ordering and orbital ordering has been found.

DOI: 10.1103/PhysRevB.68.184422 PACS number(s): 76.60.Pc

I. INTRODUCTION

The charge-transfer compound tetrakis(dimethylamine) ethylene $(TDAE)^+$-C_{60}^- has the highest transition temperature $T_c = 16$ K of all purely organic nonpolymeric ferromagnets.[1] The origin of the ferromagnetic state seems to be strongly related to the orientational ordering[2] of the C_{60}^- ions. This relation is hard to understand if the C_{60}^- ions would be spherical and the unpaired spin density uniformly distributed over the C_{60}^- sphere. A theoretical study[3] indeed yielded for undistorted C_{60}^- ions a T_c which is three orders of magnitude lower than the one observed. Recent ^{13}C NMR data[4,5] provided quantitative evidence for the occurrence of a Jahn-Teller transition in $TDAE^+$-C_{60}^-.

The room-temperature ^{13}C NMR spectra of $TDAE^+$-C_{60}^- are characteristic for fast and nearly free C_{60}^- rotations.[4] The molecular motion in fact consists of uniaxial rotations and flipping of the rotational axes of the C_{60}^- ions. Around 160 K a ^{13}C NMR linewidth transition takes place reflecting an orientational ordering transition of the C_{60}^- ions. However, the molecules still do not seem to be completely static below this transition.

A sudden increase in the inhomogeneous ^{13}C NMR linewidth of TDAE-C_{60} in the middle of the ferromagnetic phase below 10 K has been recently observed.[5] It has been interpreted[4,5] as indicating a freezeout of the pseudorotations of the axes of the Jahn-Teller distortions of the C_{60}^- ions. These distortions seem to be on the ^{13}C NMR time scale dynamic above 10 K and static below this temperature.

A quantification of the freezing dynamics of the Jahn-Teller pseudorotations still needs to be done. It is the purpose of this paper to do this. We report here on the measurements of the ^{13}C NMR line shape in TDAE-C_{60} between room temperature and 4 K as well as on a simulation of the line shape in this interval. For the entire temperature range we used the same approach by assuming both rotations and flipping of the C_{60}^- ions and pseudorotations of the axes of Jahn-Teller distortions. Correlation times for these types of motions are extracted from the comparison between experimental and computed line shapes.

The paper is organized as follows: In the second section we describe the experimental conditions. In the third section we describe in detail the theory of the ^{13}C NMR line shape in Jahn-Teller distorted C_{60}^- salts. In the fourth section we compare the experimental spectra with the theoretical spectra and extract the correlations times for the various motions involved. In the fifth section we discuss the results and present the conclusions.

II. EXPERIMENTAL DETAILS

TDAE-C_{60} single crystals were grown by a standard diffusion method[6] from 40% enriched C_{60} and were additionally characterized by ESR. After the preparation, 30–40 single crystals (with a total mass of about 30 mg) were sealed into a pyrex tube under dynamic vacuum for the NMR measurements. The sample was additionally annealed at 50 °C for 5 h. The ^{13}C NMR spectra of the well-annealed TDAE-C_{60} powder sample have been studied in a superconducting magnet with a field $B_0 = 9$ T corresponding to a Larmor frequency $\nu_0(^{13}C) = 95.6$ MHz. The ^{13}C spectra are below 150 K broader than the measurement window determined with the 90° rf pulse width 11 μs and were obtained as a sum of spectra where the resonance frequency was swept in steps of 20 kHz. To search for any additional strongly shifted ^{13}C NMR resonance we also used a frequency-sweep technique with automatic tuning of the resonance circuit in the frequency range between 63 and 73 MHz and a frequency step of 10 kHz. The magnetic field was $B_0 = 6.34$ T and $\nu_0(^{13}C) = 67.9$ MHz. An Oxford Instruments continuous flow cryostat with a temperature stability of 0.1 K has been used in the temperature range between 300 and 4 K.

III. THEORY OF THE ANISOTROPIC ^{13}C NMR LINE SHAPE IN C_{60}^- SALTS

Two types of motions will be considered to affect the ^{13}C NMR line shape in TDAE-C_{60}. The first type of the motion is physical rotations of the C_{60}^- ion. This type of motion has been studied in detail in pure C_{60}.[7–9] It involves both uniaxial rotations (characterized by a characteristic time τ_R) around the molecular threefold axes accompanied by a flipping of these axes (characterized by a characteristic time τ_F)

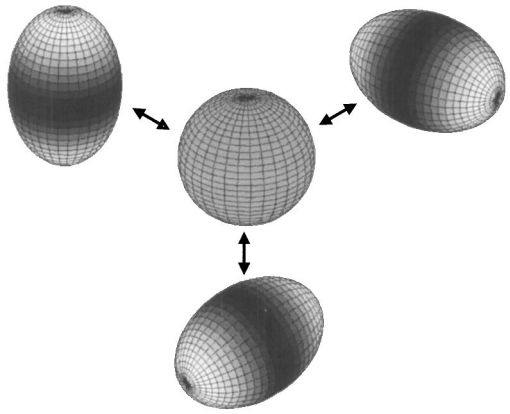

FIG. 1. A schematic picture showing Jahn-Teller pseudorotations between three mutually perpendicular distortion directions in TDAE-C_{60}.

between the symmetry allowed orientations. Below 90 K the C_{60} molecules freeze into two nearly degenerate orientations. Although the orientational potential in TDAE-C_{60} will be rather different from the one in pure C_{60} we assume that the same types of motions are taking place here here too. We assume that the physical motion of the C_{60}^- ions in TDAE-C_{60} is a combination of the uniaxial rotations and flipping of the axes of the rotations.

The second type of motion is the pseudorotation of the axes of the Jahn-Teller distortion of the C_{60}^- ion. It is well known that adding electrons to the lowest unoccupied threefold degenerate t_{1u} C_{60} molecular orbital (LUMO) should lead to a Jahn-Teller distortion of the molecule.[10] Three different nearly degenerate structures of Jahn-Teller distorted C_{60}^- ions have been identified having D_{5d}, D_{3d}, and D_{2h} symmetry.[11] In TDAE-C_{60} we shall assume the existence of the D_{2h} structure as it is compatible with the crystal symmetry. It results in a splitting of the threefold degerate t_{1u} levels into three nondegenerate states.[12] One of them, assigned as $LUMO_z$ corresponds to the beltlike charge-density distribution around the elongated z axis of the C_{60}^- ion and has a lower energy than the other two orthogonal states assigned as $LUMO_x$ and $LUMO_y$. It is therefore the ground state. Further we shall assume that the molecular z axes can be in general aligned along the three crystal directions a, b, and c. The molecular z axes can jump between these three directions with a characteristic time τ_{JT} (Fig. 1). It is this type of motion, which can dramatically affect the ^{13}C NMR line shape in view of the electron-nuclear hyperfine coupling as discussed below.

The ^{13}C NMR signal is quite generally given by the relaxation function $G(t)$ as

$$G(t)=\exp[i\omega_0 t]\left\langle \exp\left[i\int_0^t \omega'(t')dt' \right]\right\rangle, \tag{1}$$

where ω_0 is the unperturbed (time independent) ^{13}C NMR frequency and $\omega'(t')$ is the fluctuating part of the ^{13}C NMR frequency. The ^{13}C NMR spectra are then obtained by the Fourier transform of the relaxation function $G(t)$,

$$S(\omega)=\int G(t)e^{i\omega t}dt. \tag{2}$$

In TDAE-C_{60} (and other fullerides in general) the ^{13}C NMR Hamiltonian can be decomposed into two contributions. The isotropic Zeeman interaction $\mathcal{H}_Z=\gamma_C \mathbf{I}\cdot\mathbf{B}_0$ does not contribute to the ^{13}C NMR linewidth. It defines ω_0 in Eq. (1). Here γ_C is the ^{13}C giromagnetic ratio, I is the nuclear spin, and B_0 is the external magnetic field. Anisotropic contributions, which can be written in compact form as $\mathcal{H}_A=\gamma_C \mathbf{I}\cdot\underline{\underline{K}}\cdot\mathbf{B}_0$ determine the actual ^{13}C NMR line shape. Here $\underline{\underline{K}}$ is the ^{13}C anisotropic shift tensor. In C_{60}-based compounds $\underline{\underline{K}}$ can be to a very good approximation taken as an axially symmetric tensor characterized by two eigenvalues $K_\perp=\frac{1}{2}(K_{xx}+K_{yy})$ and $K_\parallel=K_{zz}$.

There are three contributions to the ^{13}C shift tensor $\underline{\underline{K}}$: the ^{13}C chemical shift tensor $\underline{\underline{\sigma}}$, the ^{13}C-electron dipolar interaction tensor $\underline{\underline{K}}^{dd}$, and the isotropic part of the electron-nuclear hyperfine coupling tensor representing the Fermi contact interaction $\underline{\underline{K}}^S$. The components of chemical shift tensor $\underline{\underline{\sigma}}$ can be in the first approximation taken from the measurements on pure C_{60}. The components of the dipolar hyperfine coupling $\underline{\underline{K}}^{dd}$ can be calculated for an electron in the carbon $2p_z$ orbital to be

$$K_\perp^{dd}=-\frac{2}{5}\frac{\mu_0}{4\pi}\hbar^2\gamma_e\gamma_C\left\langle\frac{1}{r^3}\right\rangle\frac{\langle S\rangle}{B_0}, \tag{3a}$$

$$K_\parallel^{dd}=\frac{4}{5}\frac{\mu_0}{4\pi}\hbar^2\gamma_e\gamma_C\left\langle\frac{1}{r^3}\right\rangle\frac{\langle S\rangle}{B_0}, \tag{3b}$$

where γ_e is the electron giromagnetic ratio, $\langle r^{-3}\rangle \approx 1.7a_B^{-3}$, and $\langle S\rangle$ is the expectation value for the electron spin S. The Fermi contact interaction $\underline{\underline{K}}^S$ is, on the other hand, determined by

$$K^S=\frac{2}{3}\frac{\mu_0}{\hbar}\gamma_e\gamma_C|\psi(0)|^2\frac{\langle S\rangle}{B_0}, \tag{4}$$

where $|\psi(0)|^2$ is the electron spin density at the nucleus produced by the $2s$ admixture into the $2p_z$ orbitals. If we assume that the eigenvectors for all three anisotropic tensors coincide the components of $\underline{\underline{K}}$ are simply the sum of individual contributions, i.e., $K_\parallel=\sigma_\parallel+K_\parallel^{dd}+K^S$ and $K_\perp=\sigma_\perp+K_\perp^{dd}+K^S$. While $\underline{\underline{\sigma}}$ is assumed to be more or less temperature independent, $\underline{\underline{K}}^{dd}$ and $\underline{\underline{K}}^S$ are expected to be strongly temperature dependent through the temperature dependence of $\langle S\rangle$. It is well known that for $T>T_C$ $\langle S\rangle=\chi_S B_0$ whereas for $T<T_C$ $\langle S\rangle\propto M_0$. Here χ_S is the electronic susceptibility and M_0 the spontaneous magnetization.

The ^{13}C NMR frequency $\omega'(t)$ can then be calculated as[7]

$$\omega'(\vartheta_B,\varphi_B,\vartheta,\varphi,t)=\omega_L[K_\perp+(K_\parallel-K_\perp)\cos^2\Theta(t)], \tag{5}$$

where $\Theta(t)$ is the angle between the largest principal axis of the shift tensor and the direction of the external magnetic field. $\Theta(t)$ can be expressed as

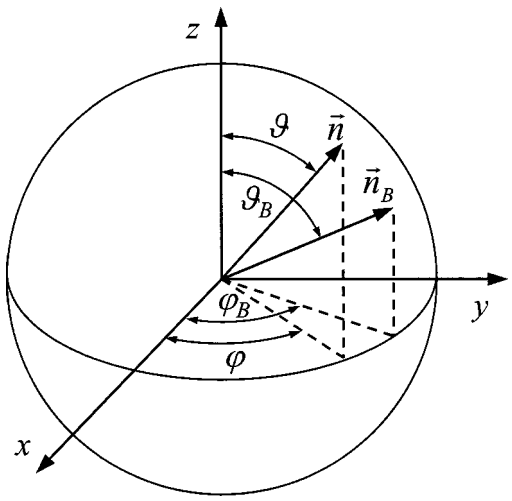

FIG. 2. Definitions of the angles ϑ_B, φ_B, which describe the orientation of the magnetic field with respect to the crystal lattice and the angles ϑ, φ describing the position of a given C atom on the C_{60}^- ion.

$$\cos\Theta(t) = \sin\vartheta_B \sin\vartheta(t)\cos(\varphi(t)-\varphi_B) + \cos\vartheta_B \cos\vartheta(t). \tag{6}$$

Here ϑ_B, φ_B describe the orientation of the magnetic field with respect to the crystal lattice whereas $\vartheta(t), \varphi(t)$ describe the position of a given carbon atom on the C_{60}^- ion at time t (Fig. 2).

Next we discuss the effect of the deviation of the charge distribution $p(\vartheta,\varphi,t)$ from the spherical one. In case of spherical symmetry of the unpaired electron spin-density distribution, all ^{13}C nuclei are equivalent and will experience the same Fermi contact shift. A Jahn-Teller distortion will make the charge distribution beltlike resulting in the fact that different carbon atoms on the C_{60}^- ion will experience different Fermi contact shifts and thus become nonequivalent. Carbon atoms on poles feel the lowest spin density while carbons on equator feel the higher spin density in accordance to the theoretical predictions.[12] If the axis of Jahn-Teller distortion changes with time, the spin density at a selected carbon site fluctuates and the hyperfine fields become time dependent. We further assume that both the parallel and the perpendicular components of the anisotropic shift tensor $\underline{\underline{K}}$ of the carbon atom at $\vartheta(t), \varphi(t)$ are modified by the same amount,

$$\delta K_{\perp,\parallel}(\vartheta,\varphi,t) = Bp(\vartheta,\varphi,t) \tag{7}$$

and

$$K_{\perp,\parallel}(\vartheta,\varphi,t) = K^0_{\perp,\parallel} + \delta K_{\perp,\parallel}(\vartheta,\varphi,t). \tag{8}$$

If Eq. (8) is inserted into Eq. (5) one obtains the ^{13}C NMR frequency for a Jahn-Teller distorted C_{60}^- ion as

$$\omega'(\vartheta_B,\varphi_B,\vartheta,\varphi,t) = \omega_L[K^0_\perp + Bp(\vartheta,\varphi,t) + (K^0_\parallel - K^0_\perp)\cos^2\Theta(t)]. \tag{9}$$

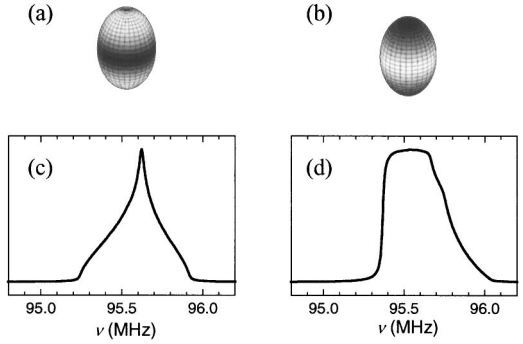

FIG. 3. Unpaired spin-density distributions on the Jahn-Teller distorted C_{60}^- ions and corresponding ^{13}C NMR line shapes: (a) A higher spin density on the equator corresponding to $p_1(\vartheta)$; (b) A higher spin density on poles corresponding to $p_2(\vartheta)$. (c) Simulated ^{13}C NMR spectra for the case (a), i.e., the $p_1(\vartheta)$ unpaired spin density. (d) Simulated ^{13}C NMR spectra for the case (b), i.e., the $p_2(\vartheta)$ unpaired spin density.

Let us now discuss a few limiting cases that emerge from the calculation of the ^{13}C NMR line shape using Eqs. (1), (2), and (9).

A. Very low temperatures

At very low temperatures the Jahn-Teller distortion is static on the NMR time scale and we can ignore the time dependence of the charge distribution function $p(\vartheta,\varphi,t)$. The ^{13}C NMR spectrum is then calculated by performing powder averaging thus taking into account all possible ^{13}C sites on the C_{60}^- sphere,

$$f(\omega) = \int\int\int \delta[\omega - \omega'(\vartheta_B,\varphi_B,\vartheta,\varphi)] \times \sin\vartheta_B \; d\vartheta_B \; d\varphi_B \sin\vartheta \; d\vartheta \; d\varphi, \tag{10}$$

where $\omega'(\vartheta_B,\varphi_B,\vartheta,\varphi)$ is defined by Eq. (9).

Various different spin-density distribution functions were tested to fit the measured ^{13}C NMR spectrum at $T = 5$ K. They can be divided into two classes: In the first the excess of the unpaired spin density is on the equator of the C_{60}^- molecule. In the second the maximum unpaired spin density is on the poles of the C_{60}^- ion. Typical representatives of these two classes are $p_1(\vartheta) = \frac{1}{3} - \cos^2\vartheta$ and $p_2(\vartheta) = \cos^2\vartheta - \frac{1}{3}$, respectively [Figs. 3(a) and (b)]. Please note that the charge distribution functions were chosen in such a way that on the average $\langle p(\vartheta)\rangle = 0$, i.e., $p(\vartheta)$ describes only the deviation of the unpaired spin density from the spherical spin-density distribution.

The spectra calculated for these two extreme cases differ qualitatively. While the spectrum for a beltlike charge-density distribution is nearly triangular and very symmetric [Fig. 3(c)]. This is not the case for the charge density having a maximum on poles [Fig. 3(d)]. Here the spectrum is asymmetric and nearly powderlike. The low-temperature ^{13}C NMR spectra should thus enable one to discriminate between the two above extreme cases. We note that the actual ^{13}C NMR line shape does depend on the details of the charge-

density distribution, i.e., on the functional form of $p(\vartheta,\varphi)$ although the general conclusions remain valid. We also tested the dependence of the ^{13}C NMR line shape on the parameter B. We note here that the parameter B measures how large the difference is between the spin density on the poles and the equator. For a very small deviation, $B\rightarrow 0$, the ^{13}C NMR spectrum approaches a powderlike form with two singularities at $K_{\perp}^{0}$ and $K_{\parallel}^{0}$. On the other hand, increasing B just broadens and emphasizes the characteristics of the two spectra presented in Figs. 3(c) and (d).

B. Intermediate temperatures

At intermediate temperatures the characteristic time for the Jahn-Teller pseudorotation $\tau_{\mathrm{JT}}\approx 1/\Delta\nu_{1/2}\approx 3$ nsec—or what is the same, the distortion of the C_{60}^{-} sphere—is comparable to the characteristic time of our ^{13}C NMR experiment given by the rigid lattice linewidth. In this case the Jahn-Teller dynamics affects the ^{13}C NMR line shape in TDAE-C_{60}. We note that the C_{60}^{-} ion itself is in this temperature range static on the ^{13}C NMR time scale, i.e., it does not perform any sort of physical reorientation. That means that $\cos^2\Theta(t)$ given by Eq. (6) is essentially time independent. The only time dependence comes through the changes in the charge-density distribution function $p(\vartheta,\varphi,t)$. As discussed in Ref. 12 the axes of the Jahn-Teller distortion can be oriented either parallel to the crystal c axis or perpendicular to the crystal c axis. At low temperatures the Jahn-Teller distortions of the C_{60}^{-} ions are frozen and one finds the spectral form discussed in previous section. However, as the temperature raises one orientation of the axis of the Jahn-Teller distortion may transform into the second one, which is perpendicular to the first one and vice versa. This results in a partial motional averaging of the otherwise ''static'' ^{13}C NMR spectra and allows us to extract the characteristic correlation times τ_{JT} from the spectra. Though the position of the ^{13}C nuclei does not change significantly (as Jahn-Teller distortions are small and of the order of 0.01 Å) the unpaired spin-density distribution on C_{60}^{-} ions—and as discussed in the previous section also the ^{13}C NMR frequency—may change dramatically. Effectively we thus have a problem of a two- or three-site exchange where the resonant frequency of the ^{13}C nuclei jumps between three different values corresponding to the three different orientations of the axis of the Jahn-Teller distortion (Fig. 1). In this case each C atom on the C_{60}^{-} ion has three different possible resonant frequencies connected with three different charge densities,

$$p_{\mathrm{I}}(\vartheta,\varphi)=\tfrac{1}{3}-\cos^2\vartheta, \tag{11a}$$

$$p_{\mathrm{II}}(\vartheta,\varphi)=\tfrac{1}{3}-(\sin\vartheta\sin\varphi)^2, \tag{11b}$$

and

$$p_{\mathrm{III}}(\vartheta,\varphi)=\tfrac{1}{3}-(\sin\vartheta\cos\varphi)^2. \tag{11c}$$

To calculate the ^{13}C NMR spectra in this temperature range we use Eqs. (1), (2), and (9) by assuming that at $t=N\tau_{\mathrm{JT}}$ $p_{\mathrm{I}}(\vartheta,\varphi)$ changes randomly to $p_{\mathrm{II}}(\vartheta,\varphi)$ or $p_{\mathrm{III}}(\vartheta,\varphi)$ and vice versa (Fig. 4). We fixed $K_{\perp}^{0}=-1100$ ppm and $K_{\parallel}^{0}$ $=2000$ ppm and varied τ_{JT} to follow the evolution of the ^{13}C NMR spectra (Fig. 5). For very short τ_{JT} values the calculated ^{13}C NMR spectra approach the powderlike line-shape characteristic for uniaxial anisotropy of the shift tensor as $\langle p(\vartheta,\varphi,t)\rangle_t=0$. However, when the reorientation of the axis of Jahn-Teller distortion freezes out, i.e., when $\tau_{\mathrm{JT}}\cdot\Delta\nu\gg 1$, the ^{13}C NMR line shape approaches the static shape discussed in the previous section. Between these two limits we have a dramatic linewidth and line-shape transition.

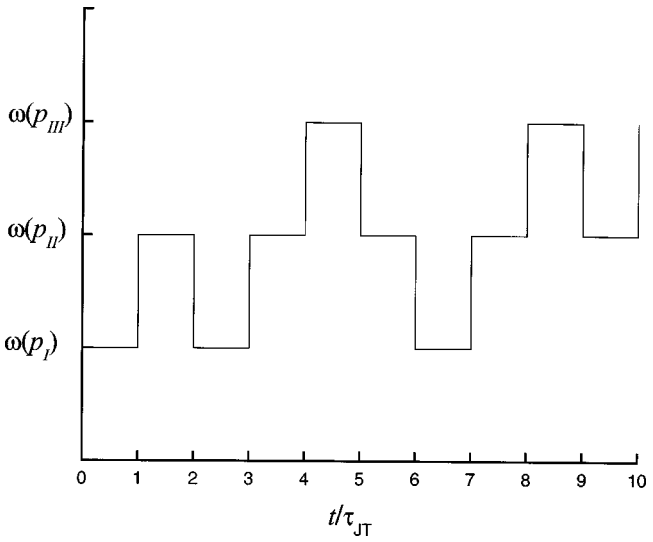

FIG. 4. Schematic dependence of the ^{13}C NMR frequency on the flipping of the Jahn-Teller distortion axes. The correlation time for the flipping is τ_{JT}.

C. High temperatures

In the ''high''-temperature regime we assume that the Jahn-Teller pseudorotations are already fast on the ^{13}C NMR time scale. In this case the effective spin density is spherical

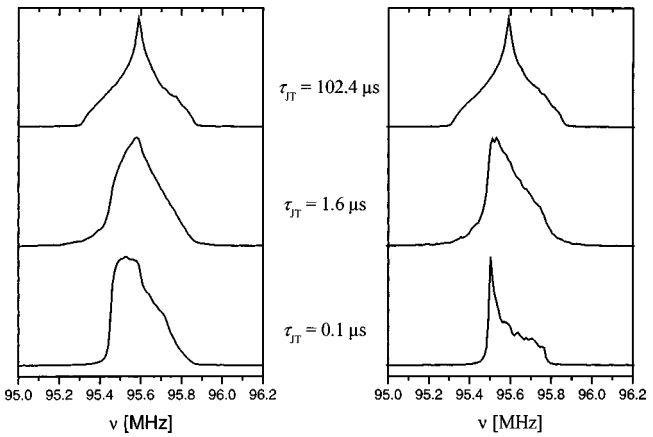

FIG. 5. Variation of the ^{13}C NMR line shape due to the reorientations of the Jahn-Teller distortion axes. Spectra on the left side were calculated by considering the reorientation of the Jahn-Teller distorted C_{60}^{-} ions between two perpendicular orientations (lets say between p_{I} and p_{II}). Spectra on the right side were calculated by considering the reorientation of the Jahn-Teller distorted C_{60}^{-} ions between all three perpendicular orientations.

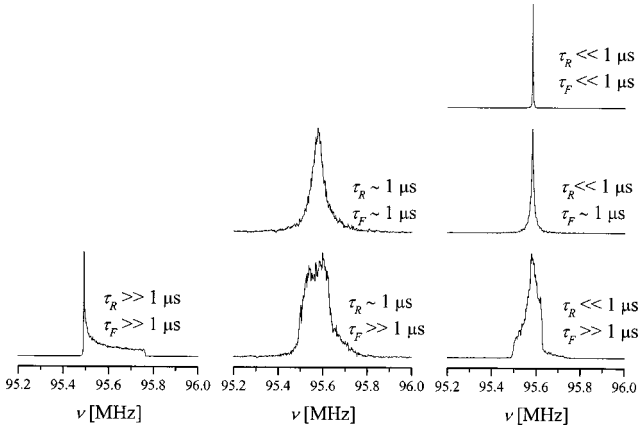

FIG. 6. Dependence of the simulated ^{13}C NMR spectra on the frequency of the uniaxial rotation and flipping of the rotational axes of the C_{60}^- ion.

as $\langle p(\vartheta,\varphi,t)\rangle_t = 0$ and one can use Eq. (5) to calculate the ^{13}C NMR spectra. The motional averaging of the ^{13}C NMR line shape is now solely due to the physical rotation of the C_{60}^- ion. The problem is now analogous to the line-shape analysis in solid C_{60}.[7] If the C_{60}^- ion performs only uniaxial reorientations, then only the azimuthal angle $\varphi(t)$ changes with time in Eq. (6). However if the molecules perform fast isotropic reorientations, which may be a result of combination of uniaxial reorientations and flipping of the axis of reorientations between several different orientations, then also the polar angle becomes time dependent $\vartheta(t)$. In the fast motion limit we need in both cases to average $\langle \cos\Theta(t)\rangle_{\vartheta(t),\varphi(t)}$. For the isotropic type of motion we predict only a very narrow Lorentzian line while for the uniaxial reorientation the anisotropy is not completely averaged out. A transition from the static to dynamic limit takes place when the spectra have to be evaluated numerically using Eqs. (1), (2), and (5). Typical spectra are shown in Fig. 6.

IV. EXPERIMENTAL RESULTS

A selection of ^{13}C NMR spectra measured between room temperature and 5 K in polycrystalline ^{13}C enriched TDAE-C_{60} is shown in Fig. 7. We mention here that ^{13}C enrichment (about 40%) is on the C_{60} sites only and that the TDAE carbons occur in natural abundance (1.108%). This ensures that the measured ^{13}C NMR spectra are due to the C_{60}^- ions only.

Above 160 K the measured ^{13}C NMR spectra are very narrow with a typical linewidth of a few kHz. The dramatic changes of the ^{13}C NMR line shape occur below 160 K. The ^{13}C NMR line suddenly becomes highly asymmetric. A shoulder first starts to grow up on the low-frequency side of the spectrum but on further cooling we find also a shoulder on the high-frequency side. At 100 K the spectrum is already very broad—it extends over 200 kHz—with a line shape reminiscent of a powderlike spectrum. On further cooling the line shape does not change appreciably except for the fact that the structure of the main peak becomes slightly more pronounced. The linewidth, however, does change significantly and at 55 K the ^{13}C spectrum extends over more than 300 kHz. Broadening of the spectra continues down to the ferromagnetic transition temperature and at 17 K, i.e., just above the transition to ferromagnetic phase, the ^{13}C NMR signal is distributed over more than 500 kHz. The line shape, however, still looks powderlike. Below 16 K a surprising transformation of the ^{13}C NMR line shape takes place. First the line becomes progressively more and more symmetric. Below 10 K a dramatic broadening of the ^{13}C NMR line takes place. It seems that at 5 K the broadening of the ^{13}C NMR line is still not saturated and that on further cooling we may get even broader lines. The ^{13}C NMR signal at this temperature extends over more than 1.4 MHz. This is more than 14 000 ppm and we are not aware of any other measured ^{13}C NMR spectrum that would be so wide. The spectrum is also rather symmetric and has an approximately triangular line shape with a slightly more pronounced center of the line.

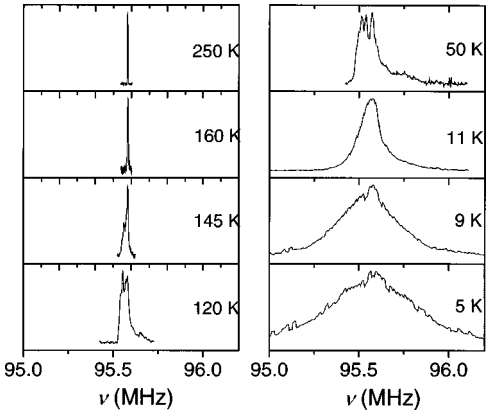

FIG. 7. The temperature dependence of selected ^{13}C NMR spectra of powdered TDAE-C_{60}.

All the changes of the ^{13}C NMR spectrum described above are even more clearly seen in the temperature dependence of the first and second moment (Fig. 8). In Fig. 8(a)

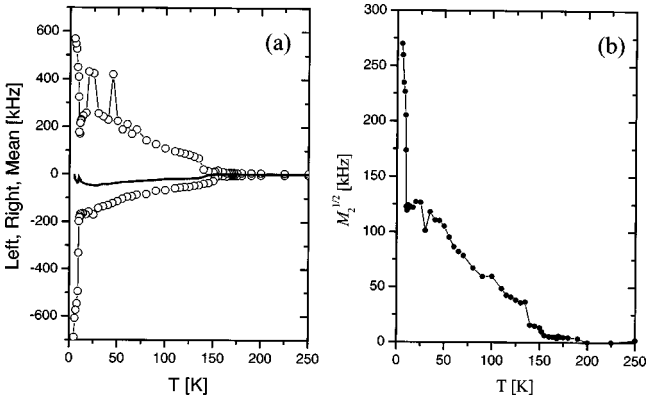

FIG. 8. (a) Temperature dependence of the two edges (circles) of the ^{13}C NMR powder spectrum of TDAE-C_{60}. The solid line shows the temperature dependence of the mean frequency, which resembles the first moment of the ^{13}C NMR line. (b) The temperature dependence of the square root of the second moment of the ^{13}C NMR line in powdered TDAE-C_{60}.

we show the temperature dependence of the two edges of the spectra and the mean frequency, which resembles the first moment of the ^{13}C NMR line. Two linewidth transitions can be deduced from the temperature dependence of the spectral edges: The first one takes place at 160 K, while the second which is even more dramatic is at 10 K. Contrary to this behavior the first moment is much less temperature dependent. While the total NMR linewidth changes by more than 1 MHz between room temperature and 5 K, the first moment changes by only 10–20 kHz. We note that when the spectra are so broad the changes of the first moment could be also artificial to some extent. The same observations come from the analysis of the second moment of the ^{13}C NMR line [Fig. 8(b)]. The second moment dramatically increases at 160 K, but never really gets saturated. In the temperature interval between 130 and 30 K the second moment follows a Curie-Weiss law with a negative Curie temperature -33 K. Between 20 and 10 K the second moment even seems to become smaller for about 15%. This is a consequence of a gradual change of the ^{13}C NMR line shape, which becomes more and more symmetric. At 10 K, however, the second moment "explodes" once again and at 5 K it reaches $\sqrt{M_2} > 270$ kHz.

V. DISCUSSION

First, let us make some general comments about the measured ^{13}C NMR spectra of TDAE-C_{60}. The fact that the shift ($\sim$188 ppm) of the ^{13}C NMR spectrum with respect to tetramethylsilane (TMS) at room temperature is rather small proves that the unpaired electron wave function in the C_{60}^- ion is principally made of $2p_z$ orbitals and that the admixture of the $2s$ orbitals is small.

Let us now describe the results of the fitting of the ^{13}C NMR spectra in the high-temperature range between room temperature and 25 K. When fitting the spectra with the formalism developed in Sec. III, we had to take into account also temperature dependence of the components of the anisotropic shift tensor $\underline{\underline{K}}$. One can deduce the temperature dependence of $\underline{\underline{K}}$ from the temperature dependence of the second moment or from the temperature dependence of the spectral edges shown in Fig. 8. If this is taken into account then a very good fit can be obtained over the entire temperature range (Fig. 9). It should be noted that the temperature dependence of the shift tensor $\underline{\underline{K}}$ shows a peak round 25 K, i.e., at the temperature of the ferromagnetic transition in the field of 9 T. It also indicates the presence of a transition around 10 K in the middle of the ferromagnetic phase. This transition could be associated with a cooperative Jahn-Teller effect and "orbital" ordering of the Jahn-Teller distorted C_{60}^- ions.

We would like to point out that the internal field distribution in TDAE-C_{60} has been accurately measured by muon spin relaxation.[13] At 4 K the mean value of the internal field is 68 G corresponding to 71 kHz for ^{13}C and the width of the internal field distribution at this temperature is 48 G corresponding to 51 kHz. This is an order of magnitude less than what we have in fact observed at 5 K. We find that the ^{13}C frequency distribution in TDAE-C_{60} extends over 720 kHz corresponding to 680 G in magnetic field units, which cannot

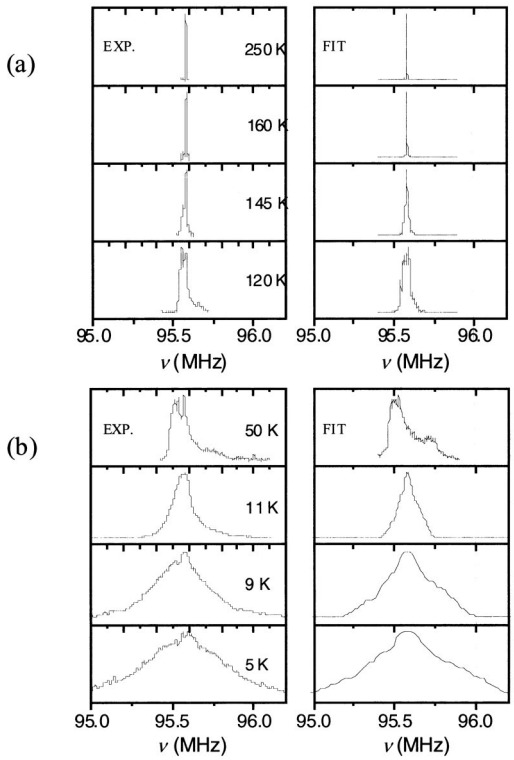

FIG. 9. A comparison between the experimental and theoretical ^{13}C NMR spectra in TDAE-C_{60}. (a) The evolution of the spectra at higher temperatures is due to the physical rotations of the C_{60}^- ions (see text for details). (b) The evolution of the spectra at low temperatures is the result of the Jahn-Teller pseudorotations of the C_{60}^- ions. In both cases (a) and (b) the left column shows the experimentally measured spectra and the right column the simulated spectra.

be explained by internal field effects. It can be, however, very well understood by the electron nuclear hyperfine interactions. In our line-shape calculations we therefore concentrated on the hyperfine electron-nuclear interactions and the motional narrowing introduced by three different processes: physical rotation of the C_{60}^- ion around the given rotational axis, flipping of this axis and Jahn-Teller pseudorotations which dominate at low temperatures and which can explain the observed linewidth and line-shape changes around 10 K.

Independent support for our interpretation comes from magnetization measurements as well as susceptibility measurements both of which show no anomalous increase around 10 K capable of explaining the observed effects.

In Fig. 10 we show the temperature dependence of the inverse spin susceptibility as measured by the X-band ESR. In the paramagnetic range the spin susceptibility follows a Curie-Weiss law $\chi = C/(T-\theta)$ with negative θ as reported earlier. We note that the second moment of the ^{13}C NMR line in the paramagnetic range between 150 and 35 K simply follows the measured spin susceptibility as suggested by Eqs. (3) and (4) but this is not the case at lower temperatures.

The fact that the ^{13}C NMR linewidth first decreases below T_c [see Fig. 8(b)] and that the line-shape changes from powderlike to more symmetric excludes the possibility that the observed changes in the ^{13}C NMR line shape come from evolution of inhomogeneties, the internal field or the spin susceptibility. We also note that at $T = 10$ K, where the ^{13}C

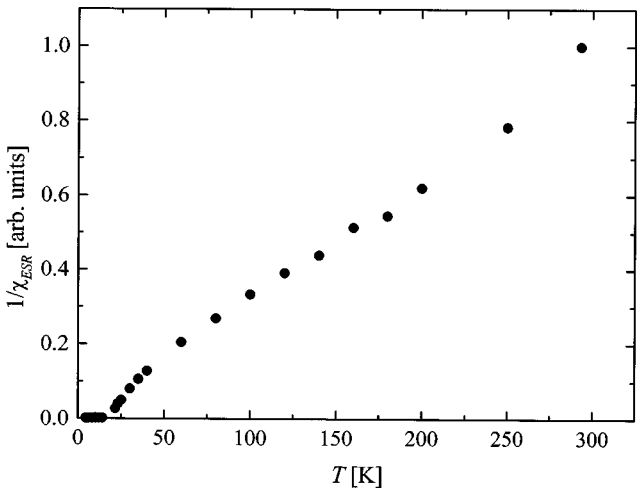

FIG. 10. The temperature dependence of the inverse spin susceptibility as measured by *X*-band EPR.

NMR linewidth increases by nearly an order of magnitude, the temperature dependence of the magnetic moment of TDAE-C_{60} shows only a change in the slope. This observation also excludes any explanation of the ^{13}C NMR lineshape development in terms of the temperature dependence of any static quantity.

The correlation times τ_R and τ_F (Fig. 11) as well as τ_{JT} (Fig. 12) can be as well extracted. Although the τ_R and τ_F values at high temperatures are associated with large error bars (the values 10^{-8} and 10^{-7} s represent just the upper limit for the correlation times), we expect that below 150 K the extracted values should be at least of the right order of magnitude. At 150 K a rather sharp orientational ordering transition of the C_{60}^- ions occurs and both τ_R and τ_F increase by more than an order of magnitude. For instance τ_R increases from 6×10^{-9} s at 150 K to 3×10^{-7} s at 135 K. The change in τ_F is even more dramatic as it increases from 2.5×10^{-7} s at 155 K to 3×10^{-4} s at 135 K. It seems that the change of τ_F is of the first order—i.e., nearly discontinuous. On the other hand, τ_R increases gradually on cooling and it seems that even at 50 K the molecules are not completely static on the ^{13}C NMR time scale. This suggests that

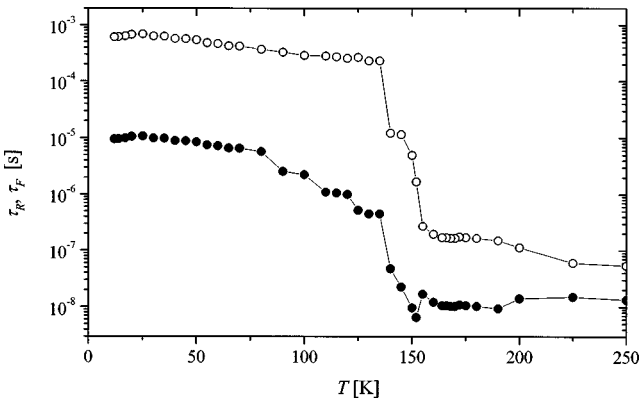

FIG. 11. Temperature dependence of the two correlation times τ_R (solid circles) and τ_F (open circles) obtained from the fits of the ^{13}C NMR spectra.

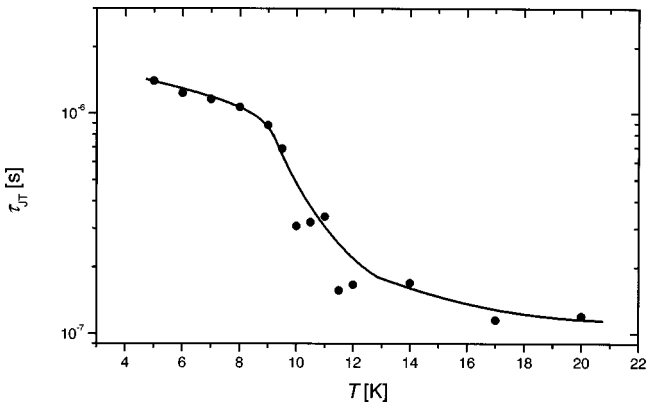

FIG. 12. Temperature dependence of the correlation times τ_{JT} obtained from the fits of the low-temperature ^{13}C NMR spectra. The solid line is a guide for the eye.

the rotational dynamics of C_{60}^- ions in the high-temperature phase is effectively nearly isotropic as it is in the fcc phase of solid C_{60}. It should be mentioned that none of the x-ray studies found any structural phase transition at this temperature. A possible reason for this is that this is a dynamic transition and that there must be a lot of disorder of the orientation of the axes of uniaxial reorientation.

As described in detail in the previous section we found large changes in the ^{13}C NMR line shape and linewidth deep in the ferromagnetic phase below 10 K. We show that these changes are connected with the slowing down of the Jahn-Teller pseudorotations. The Jahn-Teller correlation times τ_{JT} extracted from the fits of the spectra are shown in Fig. 12. They vary between $\sim10^{-7}$ s at 20 K to 10^{-6} s below 10 K. The form of the temperature dependence is similar to that expected for a freezeout transition as τ_{JT} is not simply thermally activated. It does not, however, suggest the occurrence of a sudden phase transition.

An attempt to fit the experimental spectra is shown on Fig. 9(b). Here we used unpaired spin density distributions given by Eqs. (11). We stress that the chosen $p(\vartheta,\varphi,t)$ are only a model functions and not at all unique. Regardless of that we can make some definite conclusions even from the present analysis. We noticed that at low temperatures below 10 K the calculated spectra for the Jahn-Teller distorted C_{60}^- ion reorientations do not require jumping between three but only between two orthogonal orientations. This suggests that at low temperatures in the ferromagnetic phase the Jahn-Teller distorted C_{60}^- ions indeed reorient only between two states with a perpendicular orientations of the distortion axes[14] whereas they reorient between three such states at higher temperatures (Fig. 1). In this connection one should mention that theoretical calculations have shown that perpendicular orientations of the Jahn-Teller distortion axes of two neighboring C_{60}^- ions lead to ferromagnetic coupling whereas a parallel orientation of the two distortion axes lead to antiferromagnetic coupling.

Other theoretical investigations[14] of the dependence of the exchange coupling constant on the relative orientation of the neighboring C_{60}^- ions also showed that the exchange coupling constant is very anisotropic and can change from fer-

romagnetic even to antiferromagnetic one. We can conclude that orbital ordering and spin ordering of C_{60}^{-} ions in TDAE-C_{60} are highly correlated. From the NMR results we can deduce that the Jahn-Teller determined orbital distortion axes remain dynamically disordered on the NMR time scale on cooling through $T_c = 16$ K at least down to 10 K forming a sort of an ''orbital liquid'' state. However, below $T = 10$ K a dramatic slowing down of the Jahn-Teller pseudorotational dynamics takes place leading to orbital ordering. One should mention that on the ESR time-scale this freezeout takes place around T_c.

Whether the orbital ordering is a cooperative phenomena in TDAE-C_{60} or not still remains an open question. If it is a cooperative phenomena, one can indeed apply the approach of Asai *et al.*[14] with a Hamiltonian

$$H = -\sum J_{ij}\mathbf{S}_i \cdot \mathbf{S}_j + \sum g S_i S_j O_i O_j + \sum I_{ij} O_i O_j . \tag{12}$$

Here O_i is the isospin describing the C_{60}^{-} orbital, I_{ij} is the orbital exchange constant, and J_{ij} is the Heisenberg spin-exchange constant. g represents the coupling strength between the two degrees of freedom, i.e., S and O. This Hamiltonian can describe many of the magnetic properties of TDAE-C_{60}.

If there is no cooperative orbital ordering, the Hamiltonian which describes the system is

$$H = J_{\perp} p(T) \sum \mathbf{S}_i \cdot \mathbf{S}_j + J_{\parallel}[1 - p(T)] \sum \mathbf{S}_i \cdot \mathbf{S}_j . \tag{13}$$

Here $J_{\perp}$ and $J_{\parallel}$ stand for the exchange interactions corresponding to the orthogonal or perpendicular orientations of the two Jahn-Teller distorted C_{60}^{-} ions, respectively. Most likely $J_{\perp}$ is of ferromagnetic character and $J_{\parallel}$ of antiferromagnetic character. $p(T)$ is the probability of finding the two distorted molecules in the mutual orthogonal orientations. This Hamiltonian is reminiscent of the random-exchange Hamiltonian first introduced by Soos *et al.*[15]

Still another model has been proposed by Narymbetov *et al.*[16] The magnetic behavior of the TDAE-C_{60} is here modeled in terms of a Hamiltonian for a noninteracting two-level system, where the coupling between configurational and magnetic degrees of freedom is introduced by the dependence of the exchange interaction J on the relative concentration x of configurations favoring a ferromagnetic exchange interaction. This Hamiltonian can be written as

$$H = -\sum_{i,j} J_{ij}(x)\mathbf{S}_i \mathbf{S}_j + \Delta \sum_i (\sigma_i^z + \tfrac{1}{2}). \tag{14}$$

Here Δ is the energy difference between the two configurations. $\mathbf{S}$ is the spin operator, and σ^z is the orbital operator describing the two C_{60} configurations. Here a spontaneous magnetization appears when the concentration $x = \langle \sigma_i^z + \frac{1}{2} \rangle$ is larger than a critical value. This can be understood in terms of a percolation threshold for the existence of an infinite magnetic cluster. When the magnetic energy exceeds the configurational energy difference, a ferromagnetic phase is stable below T_c. If on additional lowering of the temperature x falls below the critical value, a nonmagnetic phase could appear at low temperatures.

At this stage we cannot definitely decide which of the above Hamiltonians corresponds to the physical reality in TDAE-C_{60}. Nevertheless, it is clear that Jahn-Teller distortions of the C_{60}^{-} ions and the interplay between orbital and spin ordering are essential for the occurrence of organic ferromagnetism in TDAE-C_{60}.

[1] P. M. Allemand, K. C. Khemani, A. Koch, F. Wudl, K. Holczer, S. Donovan, G. Gruner, and J. D. Thompson, Science **253**, 301 (1991).

[2] D. Mihailovič, D. Arčon, P. Venturini, R. Blinc, A. Omerzu, and P. Cevc, Science **268**, 400 (1995).

[3] T. Sato, T. Saito, T. Yamabe, K. Tanaka, and H. Kobayashi, Phys. Rev. B **55**, 11 052 (1997).

[4] D. Arčon, J. Dolinšek, and R. Blinc, Phys. Rev. B **53**, 9137 (1996); R. Blinc, T. Apih, P. Jeglič, D. Arčon, J. Dolinšek, D. Mihailovič, and A. Omerzu, Europhys. Lett. **57**, 80 (2002).

[5] R. Blinc, P. Jeglič, T. Apih, J. Seliger, D. Arčon, J. Dolinšek, and A. Omerzu, Phys. Rev. Lett. **88**, 086402 (2002).

[6] R. Blinc, K. Pokhodnia, P. Cevc, D. Arčon, A. Omerzu, D. Mihailovič, P. Venturini, L. Golič, Z. Trontelj, J. Lužnik, and J. Pirnat, Phys. Rev. Lett. **76**, 523 (1996).

[7] R. Blinc, J. Seliger, J. Dolinšek, and D. Arčon, Phys. Rev. B **49**, 4993 (1994).

[8] R. Blinc, J. Seliger, J. Dolinšek, and D. Arčon, Europhys. Lett. **23**, 355 (1993).

[9] R. Tycko, G. Dabbagh, R. M. Fleming, R. C. Haddon, A. V. Makhija, and S. M. Zahurak, Phys. Rev. Lett. **67**, 1886 (1991).

[10] See, for instance, M. C. M. O'Brien, Phys. Rev. B **53**, 3775 (1996), and references therein.

[11] N. Koga and K. Morokuma, Chem. Phys. Lett. **196**, 191 (1992).

[12] T. Kawamoto, Solid State Commun. **101**, 231 (1997).

[13] A. Lappas, K. Prassides, K. Vavekis, D. Arcon, R. Blinc, P. Cevc, A. Amato, R. Feyerherm, F. N. Gygax, and A. Schenck, Science **267**, 1799 (1995).

[14] K. Tanaka, Y. Asai, T. Sato, T. Kuga, T. Yamabe, and M. Tokumoto, Chem. Phys. Lett. **259**, 574 (1996); Y. Asai, M. Tokumoto, K. Tanaka, T. Soto, and T. Yamabe, Phys. Rev. B **53**, 4176 (1996).

[15] S. R. Bondeson and Z. G. Soos, Phys. Rev. B **22**, 1793 (1980).

[16] B. Narymbetov, A. Omerzu, V. V. Kabanov, M. Tokumoto, H. Kobayashi, and D. Mihailovic, Nature (London) **407**, 883 (2000).